Mol. Cryst. Liq. Cryst., 1991, Vol. 199, pp. 429–452
Reprints available directly from the publisher
Photocopying permitted by license only

Printed in the United States of America

Numerical Minimization of the Landau-de Gennes Free Energy: Defects in Cylindrical Capillaries

E. C. GARTLAND, JR.†

Department of Mathematical Sciences, Kent State University, Kent, OH 44242

and

P. PALFFY-MUHORAY

Liquid Crystal Institute and Department of Physics, Kent State University, Kent, OH 44242

and

R. S. VARGA

Institute for Computational Mathematics and Department of Mathematical Sciences, Kent State University, Kent, OH 44242

(Received September 14, 1990)

In order to study the structure of defects in nematic liquid crystals, we have constructed a numerical procedure that minimizes the Landau-de Gennes free energy model. Using a new representation, a finite-element discretization, and a direct minimization scheme based on Newton's method and successive overrelaxation, this procedure determines the order parameter tensor field in three dimensions for a general physical problem with Dirichlet boundary conditions. As a sample problem, we have considered a nematic liquid crystal in a cylindrical capillary with boundary conditions that necessarily give rise to at least one defect. We find that for our parameters, two biaxial defects appear near the ends of a capillary with homeotropic alignment, and that near the center, the director is perpendicular to the axis of the cylinder.

Keywords: Numerical minimization, tensor order parameter, defects, nematic, cylindrical capillary.

†Research supported in part by NSF grant DMS-8806733.

1 INTRODUCTION

Understanding the structure of defects in liquid crystals is of fundamental and practical importance. In spite of considerable analytic[8] and numerical[1,3,4,9,12] work, unresolved questions remain. In an inhomogeneous liquid crystal, spatial variations of both the director and the scalar orientational order parameter contribute to the free energy. A consistent description is provided by the Landau-de Gennes free energy model[6] in terms of the order parameter tensor and its derivatives.

To determine the equilibrium configuration of a system, the spatially varying order parameter field which minimizes this energy must be calculated. Since the order parameter tensor contains five independent components, this calculation is formidable; we are only aware of two instances[1,12] where it has been carried out. We have undertaken to develop a general numerical procedure to carry out this minimization for a variety of geometries. As a concrete first problem we consider here a nematic confined to a cylindrical capillary with homeotropic boundary conditions and strong anchoring on the surface of the cylinder, and with oppositely directed "escape in the third dimension" director configurations at the ends in order to force the existence of defects. We have developed here a representation of the order parameter tensor which results in a simple formulation of the minimization problem. The numerical procedure is a direct minimization based on Newton's method and successive overrelaxation.

2 PROBLEM

Let $\Omega \subseteq \mathbf{R}^3$ be a bounded, connected, open region with a "sufficiently smooth" boundary, i.e., any piecewise-smooth bounded region for which the Divergence Theorem applies. For $Q(x)$ a sufficiently smooth, symmetric, traceless, 3×3, *order parameter* tensor field on Ω, the Landau-de-Gennes free-energy *density* (in the absence of surface terms and applied fields) is defined by (see, for example, Reference 10)

$$\begin{aligned} f(Q) \;:=\; & \frac{1}{2}A\,\mathrm{tr}(Q^2) - \frac{1}{3}B\,\mathrm{tr}(Q^3) + \frac{1}{4}C\,\mathrm{tr}(Q^2)^2 \\ & + \frac{1}{2}L_1 Q_{\alpha\beta,\gamma}Q_{\alpha\beta,\gamma} + \frac{1}{2}L_2 Q_{\alpha\beta,\beta}Q_{\alpha\gamma,\gamma} + \frac{1}{2}L_3 Q_{\alpha\beta,\gamma}Q_{\alpha\gamma,\beta} \end{aligned}$$

and the associated free-energy *functional* is defined by

$$F(Q) := \int_\Omega f(Q)\,.$$

Here we use the conventions that such integrals are with respect to volume, summation over repeated indeces is implied, and $Q_{\alpha\beta,\gamma}$ denotes $\partial Q_{\alpha\beta}/\partial x_\gamma$. We seek to minimize $F(Q)$ over "admissible fields" that satisfy prescribed conditions on the boundary $\partial\Omega$.

From a mathematical point of view, the appropriate "smoothness class" is $\mathscr{H}^1$, the space of tensor fields whose components have derivatives that are square integrable (i.e., $Q_{\alpha\beta,\gamma} \in L^2(\Omega)$). We let $\mathscr{H}^1_E$ denote the affine subspace (of H^1) containing all tensor fields that take on the prescribed ("essential") boundary conditions, and we denote by $\mathscr{H}^1_0$ the subspace of all $\mathscr{H}^1$ fields that *vanish* on $\partial\Omega$.

A detailed mathematical analysis of this problem will appear elsewhere. For now we mention that appropriate analogues of the scalar L^2 and H^1 inner products here are given by

$$(Q,P)_0 := \int_\Omega \mathrm{tr}(QP)\,, \qquad (Q,P)_1 := \int_\Omega \{Q_{\alpha\beta,\gamma}P_{\alpha\beta,\gamma} + \mathrm{tr}(QP)\}\,.$$

The spaces $\mathscr{L}^2$ (symmetric, traceless tensor fields with square-integrable components) and $\mathscr{H}^1$, equipped with these inner products, are Hilbert spaces.

3 SIMPLIFICATIONS

It is convenient to express the problem in dimensionless terms. We define *length* and *energy* spaces X and E by

$$X := \left(\frac{L_1 C}{B^2}\right)^{1/2}, \qquad E := \frac{B^4 X^3}{C^3},$$

dimensionless variables

$$\overline{x}_\alpha := \frac{x_\alpha}{X}, \quad \overline{A} := \frac{C}{B^2}A, \quad \overline{L}_2 := \frac{L_2}{L_1}, \quad \overline{L}_3 := \frac{L_3}{L_1},$$

and a *scaled order parameter*

$$\overline{Q} := \frac{C}{B}Q\,.$$

In terms of these, we get the dimensionless free-energy functional

$$\overline{F}(\overline{Q}) := \frac{F(Q)}{E} = \int_{\overline{\Omega}} \overline{f}(\overline{Q})\,,$$

where the dimensionless free-energy density $\bar{f}$ takes the form

$$\begin{aligned}\overline{f}(\overline{Q}) \;:=\; & \frac{1}{2}\overline{A}\,\mathrm{tr}(\overline{Q}^2) - \frac{1}{3}\mathrm{tr}(\overline{Q}^3) + \frac{1}{4}\mathrm{tr}(\overline{Q}^2)^2 \\ & + \frac{1}{2}\overline{Q}_{\alpha\beta,\overline{\gamma}}\overline{Q}_{\alpha\beta,\overline{\gamma}} + \frac{1}{2}\overline{L}_2\overline{Q}_{\alpha\beta,\overline{\beta}}\overline{Q}_{\alpha\gamma,\overline{\gamma}} + \frac{1}{2}\overline{L}_3\overline{Q}_{\alpha\beta,\overline{\gamma}}\overline{Q}_{\alpha\gamma,\overline{\beta}}\,.\end{aligned}$$

This is in the form in which we will treat this function, and to simplify notation, we will drop the overbars from the dependent and independent variables in subsequent formulas.

For the case of prescribed Dirichlet boundary conditions on the entire boundary $\partial\Omega$ (the case we consider here), we can, without loss of generality, omit either the

second or third (L_2 or L_3) gradient term. The reason for this is the following. It is a consequence of the Divergence Theorem that

$$\int_\Omega Q_{\alpha\beta,\gamma} P_{\alpha\gamma,\beta} = \int_\Omega Q_{\alpha\beta,\beta} P_{\alpha\gamma,\gamma} + \int_{\partial\Omega} \{Q_{\alpha\gamma,\beta} n_\gamma - Q_{\gamma\beta,\gamma} n_\alpha\} P_{\alpha\beta}$$

for all sufficiently smooth, symmetric tensor fields Q and P—here n denotes the outward unit normal on $\partial\Omega$. Now the condition (necessary and sufficient) for Q in $\mathcal{H}_E^1$ to be a stationary point of $F(Q)$ is (see below)

$$\int_\Omega \{\, \overline{A}\,\mathrm{tr}(QP) - \mathrm{tr}(QQP) + \mathrm{tr}(Q^2)\mathrm{tr}(QP) + Q_{\alpha\beta,\gamma} P_{\alpha\beta,\gamma} + \overline{L}_2 Q_{\alpha\beta,\beta} P_{\alpha\gamma,\gamma} + \overline{L}_3 Q_{\alpha\beta,\gamma} P_{\alpha\gamma,\beta} \,\} = 0\,, \quad \forall P \in \mathcal{H}_0^1\,.$$

The vanishing of P on the boundary eliminates the boundary integral in the previous identity and yields

$$\int_\Omega Q_{\alpha\beta,\gamma} P_{\alpha\gamma,\beta} = \int_\Omega Q_{\alpha\beta,\beta} P_{\alpha\gamma,\gamma}\,,$$

for all such fields. It follows that the stationary points are the *same* for all three of the functionals

$$\int_\Omega \left\{ \frac{1}{2}\overline{A}\,\mathrm{tr}(Q^2) - \frac{1}{3}\mathrm{tr}(Q^3) + \frac{1}{4}\mathrm{tr}(Q^2)^2 + \frac{1}{2} Q_{\alpha\beta,\gamma} Q_{\alpha\beta,\gamma} + \frac{1}{2}\overline{L}_2 Q_{\alpha\beta,\beta} Q_{\alpha\gamma,\gamma} + \frac{1}{2}\overline{L}_3 Q_{\alpha\beta,\gamma} Q_{\alpha\gamma,\beta} \right\},$$

$$\int_\Omega \left\{ \frac{1}{2}\overline{A}\,\mathrm{tr}(Q^2) - \frac{1}{3}\mathrm{tr}(Q^3) + \frac{1}{4}\mathrm{tr}(Q^2)^2 + \frac{1}{2} Q_{\alpha\beta,\gamma} Q_{\alpha\beta,\gamma} + \frac{1}{2}(\overline{L}_2 + \overline{L}_3) Q_{\alpha\beta,\beta} Q_{\alpha\gamma,\gamma} \right\},$$

and

$$\int_\Omega \left\{ \frac{1}{2}\overline{A}\,\mathrm{tr}(Q^2) - \frac{1}{3}\mathrm{tr}(Q^3) + \frac{1}{4}\mathrm{tr}(Q^2)^2 + \frac{1}{2} Q_{\alpha\beta,\gamma} Q_{\alpha\beta,\gamma} + \frac{1}{2}(\overline{L}_3 + \overline{L}_2) Q_{\alpha\beta,\gamma} Q_{\alpha\gamma,\beta} \right\}.$$

For our problem, we will discard the L_3 term. It is important to note that if a problem does not have Dirichlet boundary conditions on the *entire* boundary, then this is not necessarily justified.

From a numerical standpoint, the L_1 and the L_2 gradient terms require different treatment. The first expression simply consists of a sum of lengths squared of the gradients of the components of Q. There are no cross couplings or mixed-derivative terms involved, and the discretization that results for the system is very similar to

that for simpler, scalar equations. The L_2 term of the density, on the other hand, involves more complicated couplings and mixed derivatives.

The L_1 term contains contributions from the elastic deformations splay, twist, and bend. In the uniaxial case, the "equal elastic constant" approximation ($K_1 = K_2 = K_3$) corresponds to $L_2 = L_3 = 0$ (cf., [11, pp. 156–7]). We shall make this approximation in the numerical experiments below, although most of the following analysis applies to the more general problem.

4 A REPRESENTATION FOR Q

For analytical as well as numerical purposes, it is necessary to use a good representation for the tensor field Q, which has nine components but only five degrees of freedom because of the contraints of *symmetry* and *tracelessness*. Any five "independent" components of Q can be used. We have found it simpler (for our model problem) to use a representation based on the following. Define the five 3 by 3 matrices

$$E_1 := \begin{bmatrix} \frac{\sqrt{3}-3}{6} & & \\ & \frac{\sqrt{3}+3}{6} & \\ & & -\frac{\sqrt{3}}{3} \end{bmatrix}, \quad E_2 := \begin{bmatrix} \frac{\sqrt{3}+3}{6} & & \\ & \frac{\sqrt{3}-3}{6} & \\ & & -\frac{\sqrt{3}}{3} \end{bmatrix},$$

$$E_3 := \begin{bmatrix} 0 & \frac{\sqrt{2}}{2} & \\ \frac{\sqrt{2}}{2} & 0 & \\ & & 0 \end{bmatrix}, \quad E_4 := \begin{bmatrix} & 0 & \frac{\sqrt{2}}{2} \\ \frac{\sqrt{2}}{2} & & \end{bmatrix}, \quad E_5 := \begin{bmatrix} 0 & & \\ & 0 & \frac{\sqrt{2}}{2} \\ & \frac{\sqrt{2}}{2} & 0 \end{bmatrix}. \tag{1}$$

Here omitted entries of these matrices are zero. Any symmetric, traceless, 3×3 tensor can be uniquely written as a linear combination of these basis elements. We express Q then in the form

$$Q(x) = q_1(x)E_1 + \cdots + q_5(x)E_5 \qquad (x \in \Omega).$$

The transformation from Q to $(q_1, \ldots, q5)$ can similarly be expressed in terms of a simple linear relationship.

The basis elements (1) have the important property

$$\mathrm{tr}(E_i E_j) = \delta_{ij},$$

which helps to simplify various terms in the free-energy functional, e.g.,

$$\int_\Omega \mathrm{tr}(QP) = \int_\Omega (q_1 p_1 + \cdots + q_5 p_5)$$

and

$$\int_\Omega Q_{\alpha\beta,\gamma} P_{\alpha\beta,\gamma} = \int_\Omega (\nabla q_1 \cdot \nabla p_1 + \cdots + \nabla q_5 \cdot \nabla p_5).$$

The transformation $Q \leftrightarrow q$ provides an isometric isomorphism between $\mathscr{L}^2(\Omega)$ and $L^2(\Omega)^5$ ($:= L^2(\Omega) \times \cdots \times L^2(\Omega)$), as well as between $\mathscr{H}^1(\Omega)$ and $H^1(\Omega)^5$.

In terms of this representation, the density for the simplified model takes the form

$$\begin{aligned} f(Q) &= \frac{1}{2}Q_{\alpha\beta,\gamma}Q_{\alpha\beta,\gamma} + \frac{1}{2}\overline{A}\,\mathrm{tr}(Q^2) - \frac{1}{3}\mathrm{tr}(Q^3) + \frac{1}{4}\mathrm{tr}(Q^2)^2 \\ &= \frac{1}{2}(|\nabla q_1|^2 + \cdots + |\nabla q_5|^2) + \frac{1}{2}\overline{A}(q_1^2 + \cdots + q_5^2) \\ &\quad - \frac{1}{3}f_3(q_1, \ldots, q_5) + \frac{1}{4}(q_1^2 + \cdots + q_5^2)^2 , \end{aligned}$$

where f_3 is a homogeneous polynomial of degree three given by

$$\begin{aligned} f_3(q_1, \ldots, q_5) := \; & \frac{\sqrt{3}}{6}(q_1^3 + q_2^3) + \frac{\sqrt{3}}{2}(q_1 + q_2)(q_3^2 - q_1 q_2) \\ & + \left(-\frac{3+\sqrt{3}}{4}q_1 + \frac{3-\sqrt{3}}{4}q_2\right) q_4^2 \\ & + \left(\frac{3-\sqrt{3}}{4}q_1 + \frac{3+\sqrt{3}}{4}q_2\right) q_5^2 + \frac{3}{\sqrt{2}}q_3 q_4 q_5 . \end{aligned}$$

Our representation therefore yields a very convenient formulation for the density in this problem.

In this form, the mathematical structure of the functional, which we consider more carefully in the next section, becomes transparent. A scalar-field analogue is given by

$$\int_\Omega \left\{ \frac{1}{2}|\nabla\varphi|^2 + \frac{1}{2}\overline{A}\varphi^2 - \frac{1}{3}\varphi^3 + \frac{1}{4}\varphi^4 \right\} ,$$

whose Euler-Lagrange equation is

$$-\nabla^2\varphi + \overline{A}\varphi - \varphi^2 + \varphi^3 = 0 .$$

5 ALGEBRAIC STRUCTURE AND STATIONARITY CONDITIONS

The functional F can be written as a sum of three multi-linear forms:

$$F(Q) = a(Q,Q) + b(Q,Q,Q) + c(Q,Q,Q,Q) ,$$

where

$$a(Q,P) := \frac{1}{2}\int_\Omega \{Q_{\alpha\beta,\gamma}P_{\alpha\beta,\gamma} + \overline{L}_2 Q_{\alpha\beta,\beta}P_{\alpha\gamma,\gamma} + \overline{L}_3 Q_{\alpha\beta,\gamma}P_{\alpha\gamma,\beta} + \overline{A}\,Q_{\alpha\beta}P_{\beta\alpha}\} ,$$

and

$$b(Q,P,S) := -\frac{1}{3}\int_\Omega Q_{\alpha\beta}P_{\beta\gamma}S_{\gamma\alpha} , \quad c(Q,P,S,T) := \frac{1}{4}\int_\Omega (Q_{\alpha\beta}P_{\beta\alpha})(S_{\gamma\delta}T_{\delta\gamma}) .$$

As a function on $\mathcal{H}^1(\Omega)$ to $\mathbf{R}$, F is infinitely differentiable. The condition for Q in $\mathcal{H}^1_E$ to be a *stationary point* of F is the vanishing of the "gradient" (Fréchet derivative)

$$DF(Q)P = 0\,, \quad \forall P \in \mathcal{H}^1_0\,.$$

The stationary point Q will be a *local* (or *relative*) *minimum* if

$$D^2F(Q)(P,P) \geq 0\,, \quad \forall P \in \mathcal{H}^1_0\,;$$

it will be *isolated* (or "locally unique") if this inequality is strict for all such $P \neq 0$.

These derivatives can be easily computed in terms of the forms $a(\,\cdot\,,\cdot\,)$, $b(\,\cdot\,,\cdot\,,\cdot\,)$, and $c(\,\cdot\,,\cdot\,,\cdot\,,\cdot\,)$. Exploiting their symmetries, we get

$$DF(Q)P = 2\,a(Q,P) + 3\,b(Q,Q,P) + 4\,c(Q,Q,Q,P)$$

and

$$D^2F(Q)(P,P) = 2\,a(P,P) + 6\,b(Q,P,P) + 4\,c(Q,Q,P,P) + 8\,c(Q,P,Q,P)\,.$$

For the sake of completeness, we mention that

$$\begin{aligned} D^3F(Q)(P,P,P) &= 6\,b(P,P,P) + 24\,c(Q,P,P,P)\,, \\ D^4F(Q)(P,P,P,P) &= 24\,c(P,P,P,P)\,, \end{aligned}$$

and $D^5F = D^6F = \cdots = 0$.

Thus F has the structure of a real quartic "polynomial" on $\mathcal{H}^1$. Direct discretizations of F, via finite elements or finite differences/quadrature, will lead to finite-dimensional problems with exactly the same algebraic structure.

6 A MODEL PROBLEM IN A CAPILLARY

For concreteness and as a first application, we consider a nematic liquid crystal confined to a capillary with homeotropic anchoring. We take

$$\Omega := \{\,(r,\theta,z) \mid 0 \leq r < \overline{R},\ 0 \leq \theta < 2\pi,\ 0 < z < \overline{L}\,\}\,.$$

For boundary conditions, on the lateral surface ($r = \overline{R}$), we assume strong homeotropic anchoring, that is,

$$Q_{\alpha\beta}(x) = \frac{1}{2}(\,3n_\alpha(x)n_\beta(x) - \delta_{\alpha\beta}\,)\,,$$

where $n(x)$ denotes the outward unit normal to the surface at $x \in \partial\Omega$. At the ends of the cylinder ($z = 0$ and $z = \overline{L}$), we impose axially symmetric, oppositely directed

"escaping in the third dimension" director fields[2]: if ψ denotes the angle of inclination of the director from the axis of the cylinder, then we impose

$$\tan\frac{\psi}{2} = \begin{cases} -\dfrac{r}{R}, & z = 0 \\ \dfrac{r}{R}, & z = L. \end{cases}$$

A portion of the director field of one of our starting configurations is shown in Figure 1. It is "sliced" along the plane $\theta = 0$ (continued to $\theta = \pi$), and it clearly indicates the boundary conditions. The lengths of the line elements in this picture (and all subsequent pictures) are proportional to the largest eigenvalue of Q, and the segments are directed parallel to the corresponding eigenvector at each point. Their directions therefore represent the local director, and their lengths the local scalar order parameter S. The boundary conditions force the equilibrium field to

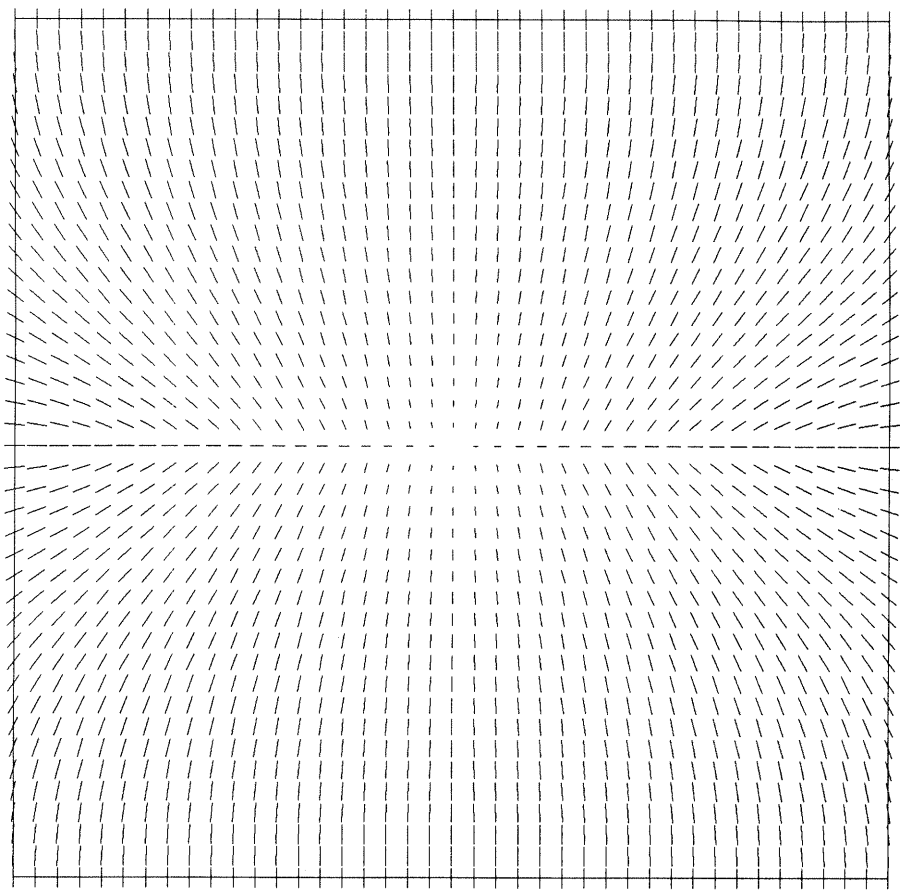

FIGURE 1 Starting configuration director field ($\theta = 0$ slice).

have at least one interior defect, and we are interested in exploring the resulting structure.

7 FINITE-ELEMENT DISCRETIZATION

We consider now the question of discretizing the problem

$$\min_{Q \in \mathcal{H}^1_E} F(Q),$$

with

$$F(Q) := \int_\Omega \left\{ \frac{1}{2} Q_{\alpha\beta,\gamma} Q_{\alpha\beta,\gamma} + \frac{1}{2}\overline{A}\,\mathrm{tr}(Q^2) - \frac{1}{3}\mathrm{tr}(Q^3) + \frac{1}{4}\mathrm{tr}(Q^2)^2 \right\},$$

where Ω is the cylinder of the previous section and the boundary conditions are as described there. Several issues need to be addressed. We have already discussed an effective approach to representing Q and handling the constraints for this problem. It is natural to use cylindrical coordinates for the independent variables. The tensor field Q can be expressed with respect to a fixed Cartesian frame of reference (since the only derivative terms in the density are $\nabla q_1, \ldots \nabla q_5$)—however, when the $\overline{L}_2$ or $\overline{L}_3$ gradient terms are present, it is necessary to use the local cylindrical-coordinate frame in order to achieve a discretization that is rotationally symmetric. We mention that transforming such gradient terms to local cylindrical coordinates complicates the functional somewhat, since these terms are invariant only under rigid-body rotations.

The Euler-Lagrange equations for the simplified model problem form a semilinear elliptic system of five partial differential equations with the following compact form:

$$-\nabla^2 q_i + \overline{A} q_i - P_i(q_1, \ldots, q_5) + (q_1^2 + \cdots + q_5^2) q_i = 0 \text{ in } \Omega, \quad i = 1, \ldots, 5, \quad (2)$$

with $q_1(x), \ldots, q_5(x)$ prescribed for $x \in \partial\Omega$. Here the P_i are homogeneous quadratic polynomials given by

$$\begin{aligned}
P_1(q_1, \ldots, q_5) &:= \frac{\sqrt{3}}{6}(q_1^2 - 2q_1q_2 - q_2^2 + q_3^2) - \frac{3+\sqrt{3}}{12}q_4^2 + \frac{3-\sqrt{3}}{12}q_5^2 \\
P_2(q_1, \ldots, q_5) &:= \frac{\sqrt{3}}{6}(-q_1^2 - 2q_1q_2 + q_2^2 + q_3^2) + \frac{3-\sqrt{3}}{12}q_4^2 - \frac{3+\sqrt{3}}{12}q_5^2 \\
P_3(q_1, \ldots, q_5) &:= \frac{\sqrt{3}}{3}(q_1 + q_2)q_3 + \frac{1}{\sqrt{2}}q_4q_5 \\
P_4(q_1, \ldots, q_5) &:= \left(-\frac{3+\sqrt{3}}{12}q_1 + \frac{3-\sqrt{3}}{12}q_2\right) q_4 + \frac{1}{\sqrt{2}}q_3q_5 \\
P_5(q_1, \ldots, q_5) &:= \left(\frac{3-\sqrt{3}}{12}q_1 - \frac{3+\sqrt{3}}{12}q_2\right) q_5 + \frac{1}{\sqrt{2}}q_3q_4 .
\end{aligned}$$

This system can be discretized via finite differences, finite elements, or other approaches.

In the case where $\overline{L}_2$ or $\overline{L}_2$ is nonzero, the form of (2) becomes more complicated. Then there is coupling in the derivative terms, there are *mixed* derivatives, the Euler-Lagrange equations are more complicated in general, and a 27-point (instead of a 7-point) stencil is required. With an eye towards future enhancements (involving the incorporation of the other gradient terms, surface terms, more general boundary conditions, and field terms), we have chosen to discretize the free-energy functional directly using a finite-element procedure, which we now briefly describe.

The cylinder Ω is partitioned into geometric "elements"

$$\Omega_{jkl} := \{ (r, \theta, z) \mid \theta_j < \theta < \theta_{j+1}\,,\ r_k < r < r_{k+1}\,,\ z_l < z < z_{l+1} \}\,,$$

for $j = 0, \ldots, J-1$, $k = 0, \ldots, K-1$, and $l = 0, \ldots, L-1$, where

$$0 = \theta_0 < \theta_1 < \cdots < \theta_J = 2\pi\,, \quad 0 = r_0 < r_1 < \cdots < r_K = \overline{R}\,,$$

and

$$0 = z_0 < z_1 < \cdots < z_L = \overline{L}\,.$$

This gives JKL elements and $(JK + 1)(L + 1)$ nodes. There are two different kinds of elements: "wedge" type (case $k = 0$) with 6 nodes and edges along the axis of the cylinder and "shell" type (case $k = 1, \ldots, K-1$) with 8 nodes.

Because of the "connectivity" of the nodes along the cylinder axis to the entire innermost ring ($r = r_1$, $k = 1$), it is natural to order/index the nodes with respect to θ (or j), then r (or k), then z (or l). This gives rise to global finite-element matrices with a block-tridiagonal structure, each block corresponding to all mesh points in a given z-plane.

We use tensor-product trilinear basis functions. Denote $\Delta\theta_j := \theta_j$, with similar expressions for Δr_k and Δz_l. Define the piecewise-linear "hat functions"

$$\Theta_j(\theta) := \begin{cases} \dfrac{\theta - \theta_{j-1}}{\Delta\theta_{j-1}}\,, & \theta_{j-1} \le \theta \le \theta_j \\ \dfrac{\theta_{j+1} - \theta}{\Delta\theta_j}\,, & \theta_j \le \theta \le \theta_{j+1} \\ 0\,, & \text{otherwise}\,. \end{cases}$$

The functions $R_k(r)$ and $Z_l(z)$ are defined in analogous fashion. The "interpolating basis" functions

$$\tilde{\varphi}_l(r, z) := R_0(r) Z_l(z)\,, \quad l = 0, \ldots, L\,,$$

and

$$\varphi_{jkl}(r, \theta, z) := R_k(r)\Theta_j(\theta) Z_l(z)\,,$$

$j = 0, \ldots, J-1$, $k = 1, \ldots, K$, and $l = 0, \ldots, L$, then have the property that each has the value *one* at a single distinct node and vanishes at all the other

nodes. These functions also have the desirable property of being *locally supported*, that is, identically *zero* outside some small region.

We seek a finite-element approximation to the tensor field Q in the form

$$Q(r,\theta,z) \cong Q^h(r,\theta,z) = \sum_{i=1}^{5}\sum_{l=0}^{L}\left\{\tilde{q}^h_{il}\,\tilde{\varphi}_l(r,z)E_i + \sum_{j=0}^{J-1}\sum_{k=1}^{K} q^h_{ijkl}\,\varphi_{jkl}(r,\theta,z)E_i\right\}.$$

Any such Q^h is in $\mathcal{H}^1$ and can be made to satisfy the essential boundary conditions (at least to second-order accuracy) by appropriately fixing the scalar coefficients associated with the boundary nodes.

A measurement of the fineness of our partition is given by

$$h := \max_{j,k,l}\{\overline{R}\Delta\theta_j, \Delta r_k, \Delta z_l\}.$$

Let $S^h \subset \mathcal{H}^1$ denote the (finite-dimensional) linear subspace spanned by our basis functions; let $S^h_E \subset S^h$ denote the affine subspace of all functions that interpolate to the boundary data; and let $S^h_0 \subset S^h$ denote those functions that vanish on the boundary. Our computational problem then is to determine

$$\min_{Q^h \in S^h_E} F(Q^h).$$

This is a large sparse unconstrained minimization problem. It has on the order of $5JKL$ unknowns—five degrees of freedom at each interior mesh point. In the next section, we discuss an iterative procedure to accomplish this minimization. We first mention some properties of the discrete functional $F(Q^h)$.

Let $\mathbf{q}_h = (q^h_\mu)_{\mu=1}^N$ denote some natural ordering of the coefficients $\tilde{q}^h_{il}$ and q^h_{ijkl}, and let $\Phi_\mu(r, \theta, z)$ denote the similarly ordered basis functions $\tilde{\varphi}_l(r, z)E_i$ and $\varphi_{jkl}(r, \theta, z)E_i$. Then the quadratic part of $F(Q^h)$ takes the form

$$\mathbf{q}_h^T A^h \mathbf{q}_h = q^h_\mu A^h_{\mu\nu} q^h_\nu,$$

where

$$A^h_{\mu\nu} := a(\Phi_\mu, \Phi_\nu).$$

This "global finite-element matrix" can be assembled from local stiffness and mass matrices. These local matrices (which just involve integrals over a single element) are either 30×30 or 40×40, depending on whether it is a "wedge" or a "shell" type element. There are simplifications because of our representation for Q and because of the tensor-product nature of the geometry and basis functions. However these matrices are large, and there are many integrals to be evaluated. We have found that using a symbolic computing package ("vaxima" in our case) was helpful for this purpose.

It becomes too costly to treat the contribution to $F(Q^h)$ from the $b(\cdot\,,\cdot\,,\cdot\,)$ and $c(\cdot\,,\cdot\,,\cdot\,,\cdot\,)$ forms in this "consistent" way, viz.,

$$b(Q^h, Q^h, Q^h) = \sum_{\mu,\nu,o=1}^{N} q_\mu^h q_\nu^h q_o^h \, b(\Phi_\mu, \Phi_\nu, \Phi_o)\,;$$

"mass lumping" is recommended. This replaces exact integrals over generic wedge and shell elements $e_1 := \{0 < r < \Delta r,\ 0 < \theta < \Delta\theta,\ 0 < z < \Delta z\}$ and $e_2 := \{r_0 < r < r_0 + \Delta r,\ 0 < \theta < \Delta\theta,\ 0 < z < \Delta z\}$ by quadrature rules:

$$\int_{e_1} f \cong (f_1 + \cdots + f_6)\frac{\Delta r^2 \Delta\theta \Delta z}{12}$$

and

$$\int_{e_2} f \cong \{(3r_0+\Delta r)(f_1+f_2+f_5+f_6)+(3r_0+2\Delta r)(f_3+f_4+f_7+f_8)\}\frac{\Delta r\Delta\theta\Delta z}{24}\,.$$

Here the nodes have been ordered in the natural (increasing θ, then r, then z) way.

This maintains the same degree of approximation in the discretization, and it eliminates the cross-coupling of different nodes in expressions of the form $b(\Phi_\mu, \Phi_\nu, \Phi_o)$ and $c(\Phi_\mu, \Phi_\nu, \Phi_o, \Phi_\pi)$. In the lumped-mass approximation, these forms simply contribute only to the 5×5 diagonal blocks.

8 MINIMIZATION

Our problem is originally posed as a minimization problem, and we have attacked it directly as such (rather than dealing with the Euler-Lagrange equations). It is natural to use Newton's method (applied to the gradient equations) to approximate the local stationary points since the exact gradients and Hessians are easy to construct here—the algebraic structure of the discrete "lumped-mass" functional

$$F^h(Q^h) := a(Q^h, Q^h) + b^h(Q^h, Q^h, Q^h) + c^h(Q^h, Q^h, Q^h, Q^h)$$

(where $b^h(\cdot\,,\cdot\,,\cdot\,)$ and $c^h(\cdot\,,\cdot\,,\cdot\,,\cdot)$ denote the lumped-mass approximations to $b(\cdot\,,\cdot\,,\cdot\,)$ and $c(\cdot\,,\cdot\,,\cdot\,,\cdot\,)$) is identical to that of $F(Q)$.

A basic Newton step, given the current approximate solution $Q^h \in S_E^h$, is to solve the linear system

$$D^2F^h(Q^h)(\Delta Q^h, P^h) = -DF^h(Q^h)P^h\,, \quad \forall P^h \in \mathcal{S}_0^h$$

for $\Delta Q^h \in S_0^h$ and then update:

$$Q^h \leftarrow Q^h + \Delta Q^h\,.$$

This is based on the local quadratic model

$$F^h(Q^h + \Delta Q^h) \cong F^h(Q^h) + DF^h(Q^h)\Delta Q^h + \frac{1}{2}D^2F^h(Q^h)(\Delta Q^h, \Delta Q^h),$$

which is minimized by the solution above if the Hessian $D^2F(Q^h)$ is positive definite.

Now this requires that a large sparse linear system of equations must be solved for the components of ΔQ^h. It is most efficient to solve this by some iterative procedure—a second ("inner") iteration. Various questions arise: how accurately should this linear system be solved before doing the Newton update, what if $D^2F(Q^h)$ is not positive definite, etc. The procedure we chose to implement (given time constraints and the "first-effort" nature of the project) is known as *One-Step Block SOR-Newton*. It proceeds as follows.

Successive sweeps are made through the mesh. At each mesh point, one step of the minimization is made over the five unknowns at that point (augmenting the 5 $\times$ 5 Hessian along its diagonal if necessary to force it to be positive definite). So if we let $g(q_1, \ldots, q_5)$ denote the discrete free-energy functional as a function of the five generic nodal unknowns $q_1, \ldots, q_5$, then we solve the system

$$(\nabla^2 g(q_1, \ldots, q_5) + \sigma I)\Delta q = -\nabla g(q_1, \ldots, q_5)$$

and then update

$$q \leftarrow q + \omega \Delta q .$$

Here σ and ω are augmentation and overrelaxation factors.

This algorithm was used to perform the numerical experiments described in the next section. Although the algorithm is robust, it is slow. Several enhancements are planned, and we plan to carry out a detailed numerical analysis of these in a subsequent paper.

9 NUMERICAL RESULTS

We performed several numerical simulations for the capillary problem using the scheme described above. We report our results for problems with parameters tabulated below. All calculations were done on the CRAY Y-MP8/864 at the Ohio Supercomputer Center. No effort has been made yet to analyze and enhance the performance of the code on this machine (other than the optimization done by the CRAY Fortan compiler). Starting configurations were taken to be either (1) a field of *zero* tensors throughout the interior ("isotropic" initialization) or (2) an ad hoc field constructed to qualitatively resemble a single point defect at the center ("point defect" initialization) which is pictured in Figure 1, or (3) primitive continuation from a previously computed field at a nearby temperature.

TABLE I

Problem Parameters for Numerical Experiments

radius	20
length	40
r mesh lines	40
θ mesh lines	8
z mesh lines	80
unknowns	123,635
$\overline{A}$ ("temperature")	$-.2, -.1, \ldots, .3$

We strived for an accuracy of three to four digits. The iteration was terminated when the seventh digit of $F^h(Q^h)$ had settled down and the gradient $DF^h(Q^h)$ had reached an acceptably small tolerance. Computing times ranged from around 15 cpu minutes to 1.5 cpu hours. The slowest times were in the low-temperature simulations where the solution that had been continued from the "isotropic" initialization became unstable and the "point-defect" initialization was also very far from the eventual fully three-dimensional biaxial solution field. Summary information and accompanying figures appear below.

The solutions for $\overline{A} = .3$, .2, and .1, and .0 are essentially axially symmetric and consist of smaller and smaller isotropic cores at positions removed from the boundary where order is rigidly imposed. This solution loses its stability between .0 and $-.1$, where a truly three-dimensional (*not* axially symmetric) biaxial solution emerges. The distinction between these two solutions is well illustrated by the behavior of the three eigenvalues of Q^h along the axis of the cylinder.

10 CONCLUDING REMARKS

These results require some interpretation and some further exploration. The high-temperature solution is distinguished by the fact that it possesses a dominant eigenvalue *pair*. The eigenspace of this pair is a plane parallel to the xy-plane. If we consider the unique (nondegenerate) eigenvector to correspond to the diretor, then this configuration may be viewed as a uniaxial nematic with a *negative* order parameter. Since all the eigenvalues are small, this inner region is nearly isotropic. As the temperature is lowered, the pair of eigenvalues separate indicating the emergence of a preferred direction in this plane. As we further lower the temperature, we see what appears to be an abrupt transition in the middle of the sample to a uniaxial configuration with the director normal to the symmetry axis of the cylinder.

For this configuration, boundary conditions require the director to change direction by 90 degrees between the center and the ends of the cylinder. Rather than by a continuous rotation of the director, this is accomplished by one of the smaller eigenvalues becoming dominant and its associated eigenvector assuming the role of the director. In the region where this interchange of dominant eigenvalues takes

TABLE II

$\bar{A} = .3$

initialization	isotropic
$F(Q_{\text{init}})$	17,661.55
$F(Q_{\text{final}})$	4,140.47
$\|\|DF(Q_{\text{init}})\|\|_\infty$	.47(2)
$\|\|DF(Q_{\text{final}})\|\|_\infty$	.11(-3)

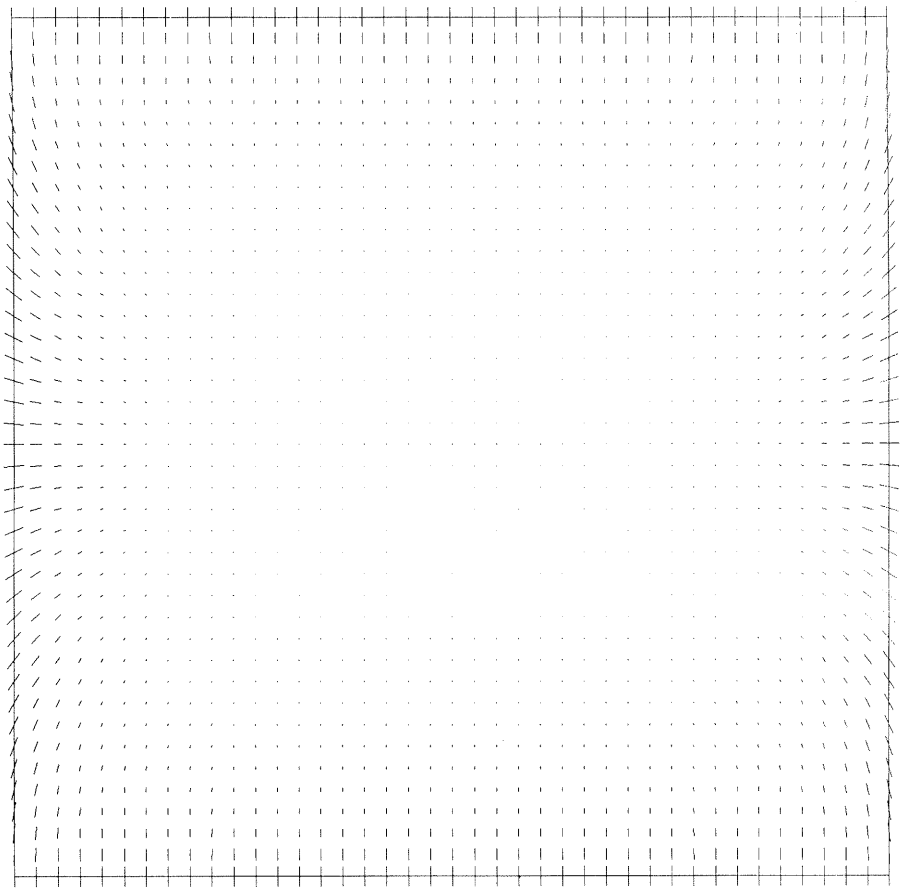

FIGURE 2 $\bar{A} = .3$.

TABLE III

$\bar{A} = .2$

initialization	cont. ($\bar{A} = .3$)
$F(Q_{\text{init}})$	3,708.87
$F(Q_{\text{final}})$	3,685.63
$\|DF(Q_{\text{init}})\|_\infty$	.32(0)
$\|DF(Q_{\text{final}})\|_\infty$	.20(-3)

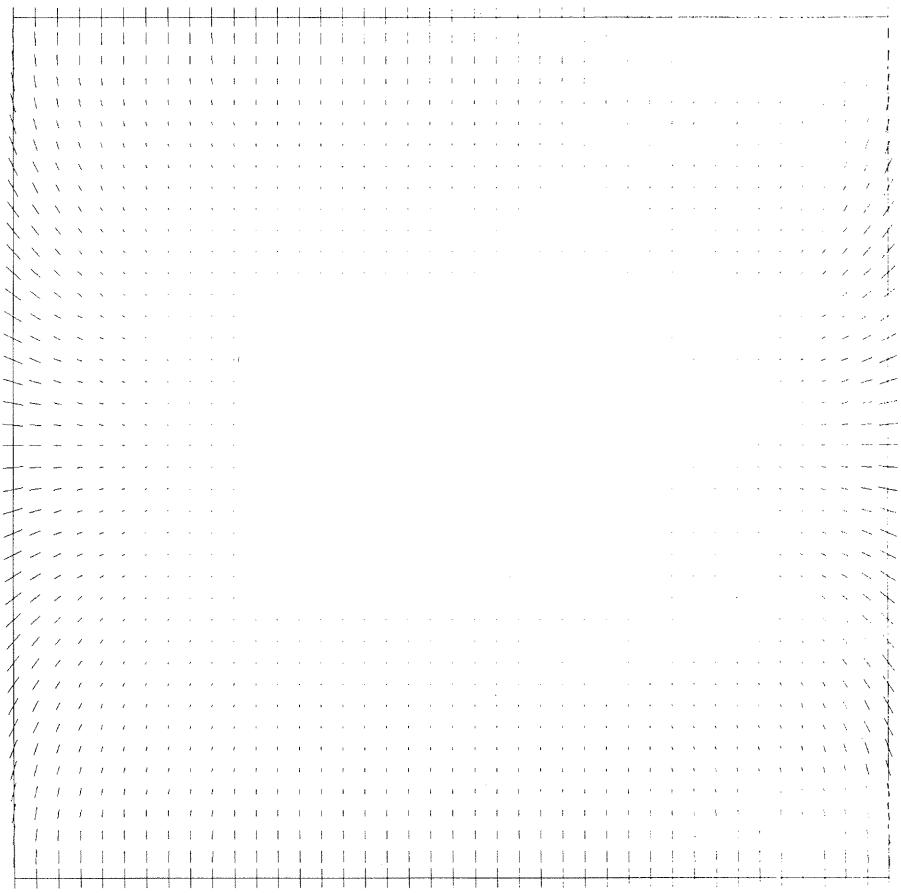

FIGURE 3 $\bar{A} = .2$.

TABLE IV

$\bar{A} = .1$

initialization	cont. ($\bar{A} = .2$)
$F(Q_{\text{init}})$	3,204.60
$F(Q_{\text{final}})$	3,170.47
$\|DF(Q_{\text{init}})\|_\infty$	.32(0)
$\|DF(Q_{\text{final}})\|_\infty$	.27(-3)

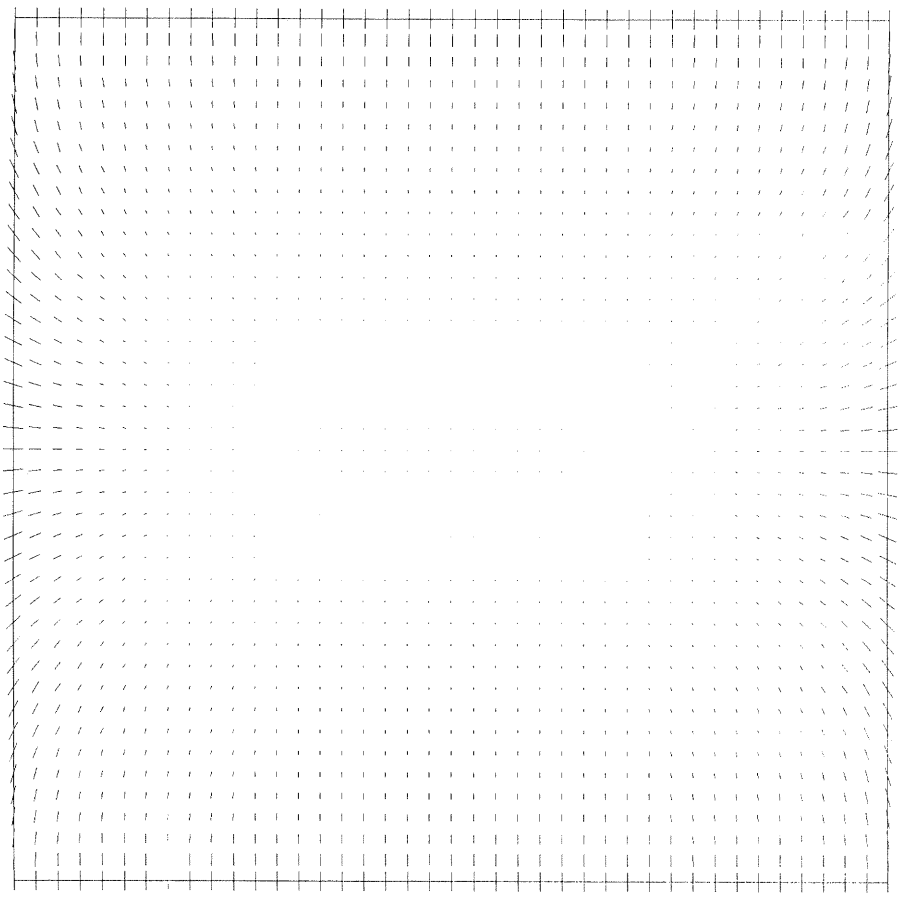

FIGURE 4 $\bar{A} = .1$.

TABLE V

$\bar{A} = .0$

initialization	cont. ($\bar{A} = .1$)
$F(Q_{\text{init}})$	2,615.42
$F(Q_{\text{final}})$	2,560.15
$\|DF(Q_{\text{init}})\|_\infty$	.32(0)
$\|DF(Q_{\text{final}})\|_\infty$	.22(-3)

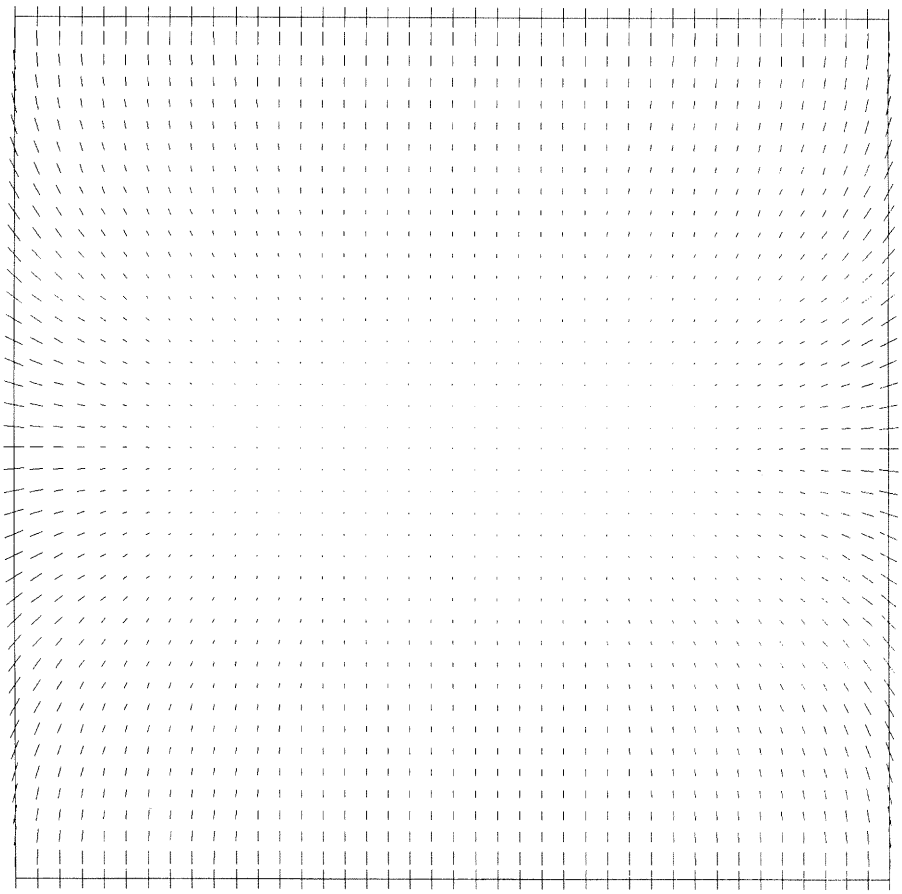

FIGURE 5 $\bar{A} = .0$.

TABLE VI

$\bar{A} = -.1$

initialization	pt. defect
$F(Q_{\text{init}})$	3,578.99
$F(Q_{\text{final}})$	1,774.20
$\|\|DF(Q_{\text{init}})\|\|_\infty$	.31(1)
$\|\|DF(Q_{\text{final}})\|\|_\infty$	.26(-3)

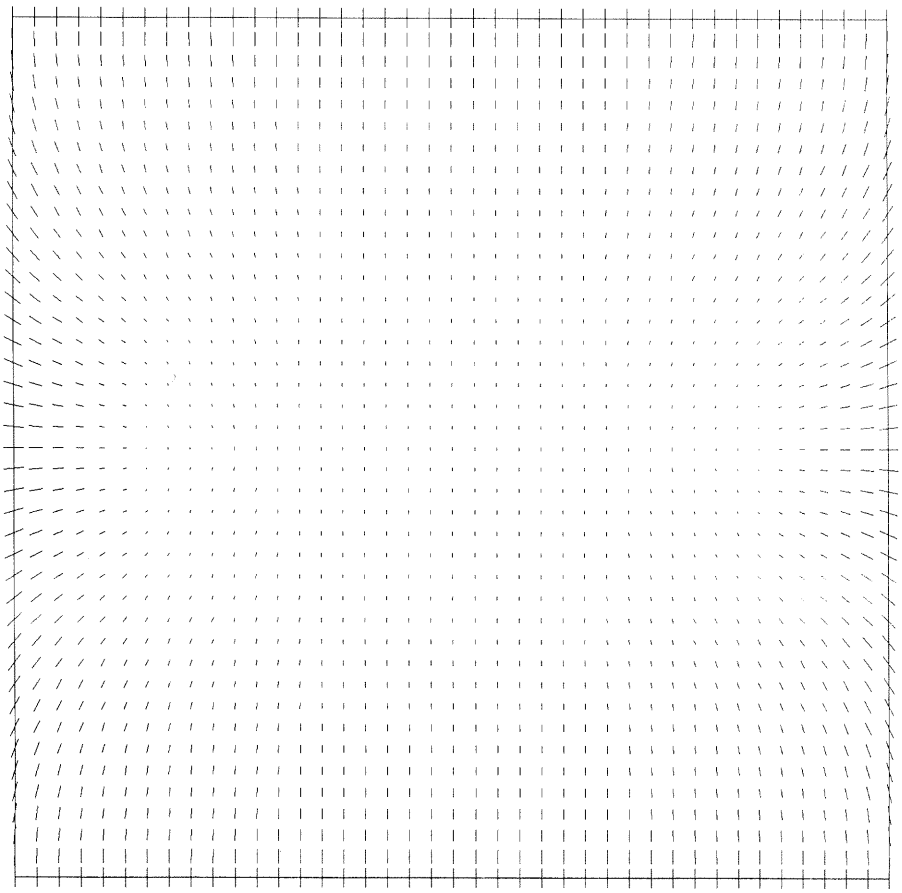

FIGURE 6 $\bar{A} = -.1$.

TABLE VII

$\bar{A} = -.2$

initialization	cont. ($\bar{A} = -.1$)
$F(Q_{\text{init}})$	872.73
$F(Q_{\text{final}})$	755.53
$\|\|DF(Q_{\text{init}})\|\|_\infty$	.33(0)
$\|\|DF(Q_{\text{final}})\|\|_\infty$	.46(-4)

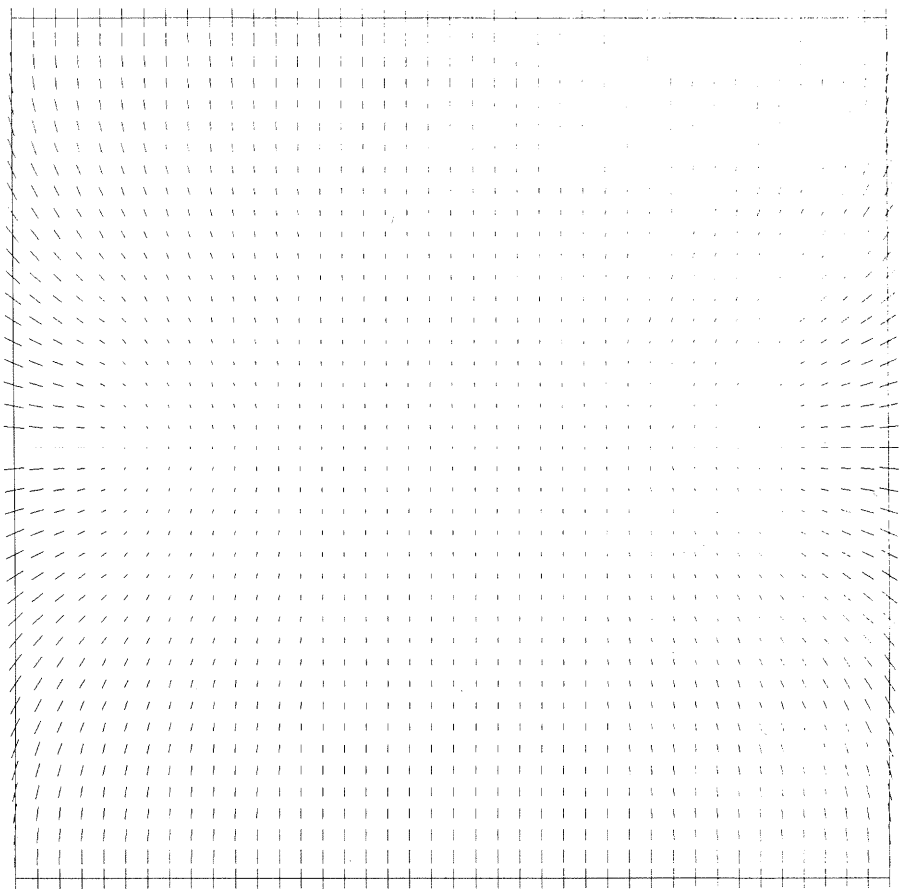

FIGURE 7 $\bar{A} = -.2$.

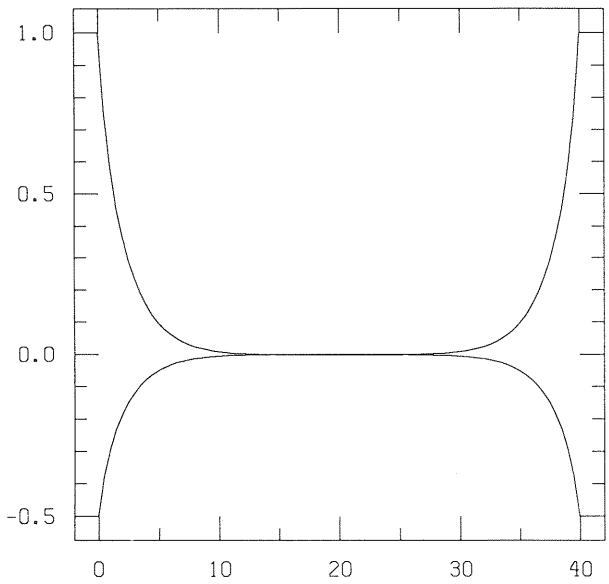

FIGURE 8 Eigenvalues ($\bar{A} = .3$).

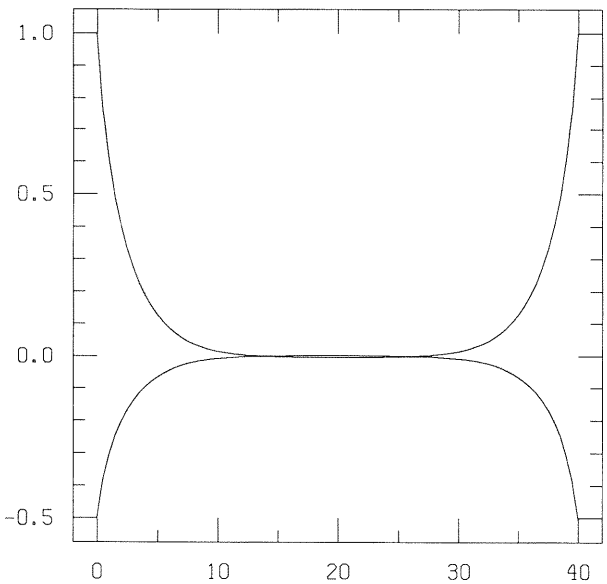

FIGURE 9 Eigenvalues ($\bar{A} = .2$).

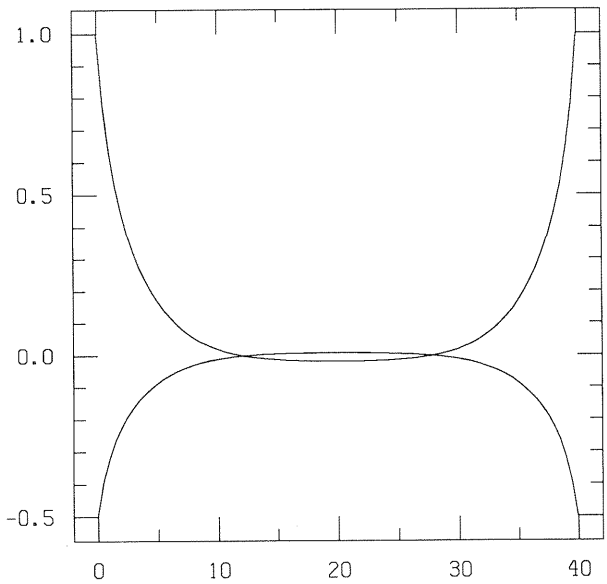

FIGURE 10 Eigenvalues ($\bar{A} = .1$).

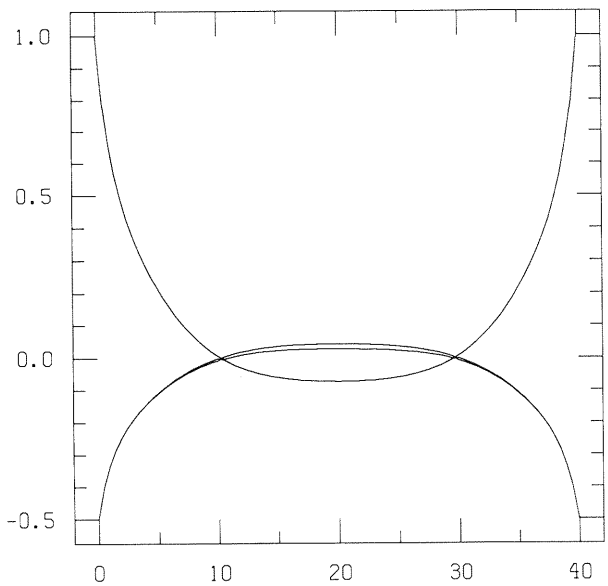

FIGURE 11 Eigenvalues ($\bar{A} = .0$).

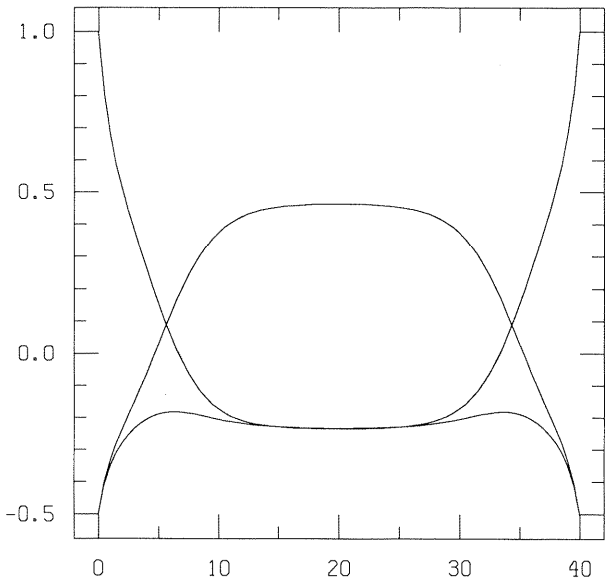

FIGURE 12 Eigenvalues ($\bar{A} = -.1$).

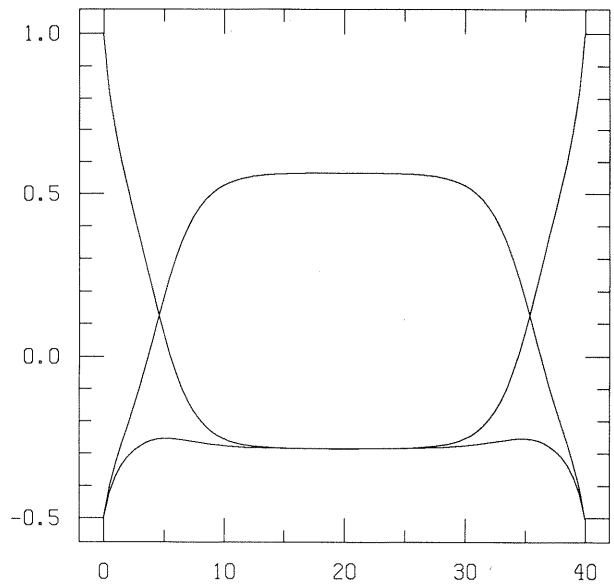

FIGURE 13 Eigenvalues ($\bar{A} = -.2$).

place, the system is strongly biaxial. Similar behavior was observed in the vicinity of a disclination of strength 1/2 by Sluckin in Reference 12.

This low-temperature solution is three-dimensional, *not* axially symmetric, despite the fact that the geometry and boundary data are completely symmetric about the axis of the cylinder. Because of the rotational symmetry of the solution, we actually get an infinite family of solutions here. This nonuniqueness (and associated non-positive-definiteness of the Hessian $D^2F(Q^h)$) certainly contributes to the degradation of the convergence rate of our iterative procedure.

We intend to explore this problem further. Improved visualization techniques are needed. It is also of interest to carefully resolve the transition from the high-temperature solution to the family of three-dimensional solutions and determine any "overlap" temperature range where both are stable or meta-stable. We also intend to consider the effect of different sizes of cylindrical capillaries and different ratios of radii to lengths. These factors have been found in other types of simulations and experiments to influence the number and distribution of defects (see References 5, 7 and 13).

Further enhancements that are planned include the addition of other gradient terms to the free-energy density, the addition of surface terms (and allowance for weak anchoring), and the incorporation of electric and magnetic field effects. We also intend to include periodic boundary conditions at the ends of the cylinder and to consider other geometries.

Enhancements of the numerical procedures will mainly be concerned with improving the convergence properties of the iterative scheme. One-step minimizations over larger blocks (entire z slices, for example) will be implemented, as will the mechanism to relax on multiple levels of coarse to fine meshes. In appropriate settings, such *multi-level* procedures enjoy essentially optimal convergence properties (in the sense that the work required to iterate to convergence grows linearly with the number of unknowns). An improved continuation procedure will be utilized to follow a solution branch parametrized by the temperature $\overline{A}$. Another numerical issue that requires addressing is the implementation of procedures to cope with the singularity of the Hessian at the three-dimensional solutions families.

References

1. D. W. Berreman, AT&T Bell Laboratories Technical Report ("Order and biaxiality variation in disclinations," 1985).
2. P. Cladis and M. Kleman, *J. Phys.*, **33**, 591 (1972).
3. R. A. Cohen, Ph.D. Thesis, University of Minnesota, Minneapolis, Minnesota, 1988.
4. J. L. Ericksen and D. Kinderlehrer (Eds.), *Theory and Applications of Liquid Crystals* (Springer-Verlag, New York, 1987).
5. J. H. Erdmann, S. Žumer and J. W. Doane, *Phys. Rev. Lett.*, **64**, 1907 (1990).
6. P. G. deGennes, *The Physics of Liquid Crystals* (Oxford Univ. Press, New York, 1974).
7. A. Golemme, S. Žumer, D. W. Allender and J. W. Doane, *Phys. Rev. Lett.*, **61**, 2937 (1988).
8. M. Kleman, *Points, Lines and Walls* (Wiley, New York, 1983).
9. S.-Y. Lin and M. Luskin, *SIAM J. Numer. Anal.*, **26**, 1310 (1989).
10. L. Longa, D. Monselesan and H.-R. Trebin, *Liq. Cryst.*, **2**, 769 (1987).
11. E. B. Priestly, P. J. Wojtowicz and P. Sheng (Eds.), *Introduction to Liquid Crystals* (Plenum Press, New York, 1976).
12. N. Schopohl and T. J. Sluckin, *Phys. Rev. Lett.*, **59**, 2582 (1987).
13. I. Vilfan, M. Vilfan and S. Žumer, 13th ILCC Proceedings, to be published.